Research on Control Strategy of Grid-connected Brushless Doubly-fed Wind Power System Based on Virtual Synchronous Generator Control

Shuai Liang, Shi Jin, *Member, IEEE*, and Long Shi

***Abstract*—The brushless doubly-fed wind power system based on conventional power control strategies lacks 'inertia' and the ability to support grid, which leads to the decline of grid stability. Therefore, a control strategy of brushless doubly-fed reluctance generator (BDFRG) based on virtual synchronous generator (VSG) control is proposed to solve the problem in this paper. The output characteristics of BDFRG based on VSG are similar to a synchronous generator (SG), which can support the grid frequency and increase the system 'inertia'. According to the mathematical model of BDFRG, the inner loop voltage source control of BDFRG is derived. In addition, the specific structure and parameter selection principle of outer loop VSG control are expounded. The voltage source control inner loop of BDFRG is combined with the VSG control outer loop to establish the overall architecture of BDFRG-VSG control strategy. Finally, the effectiveness and feasibility of the proposed strategy are verified in the simulation.**

***Index Terms*—Virtual synchronous generator, Brushless doubly-fed relutance generator, Grid support ability, Voltage source control.**

I. INTRODUCTION

THE brushless doubly-fed reluctance generator is improved from doubly fed induction generator (DFIG), so it inherits many advantages of DFIG. For example, it is easy to realize variable speed constant frequency operation, can flexibly control active power and reactive power, the cost of the motor is moderate, and the converter with small capacity. Different from DFIG, BDFRG has no brush and slip ring in structure, which significantly improves the reliability of the system [1]–[3]. In addition, due to the large leakage inductance of BDFRG, it has good performance in low voltage ride through [4]. Compared with brushless doubly fed induction generator, the control system of BDFRG has less dependence on parameters and simple control structure. Therefore, BDFRG is suitable for high reliability wind power generation.

At present, many control strategies for BDFRG have been proposed, including vector control [6]–[8], direct torque control [9],[10] and direct power control [11]. Vector control has the advantages of fast response and fixed switching frequency, but PI controller needs to be adjusted accurately. Direct torque control and direct power control focus on improving the response speed, but variable switching frequency limits its advantages. The direct power control based on model prediction has good response speed, fixed switching frequency and does not require PI regulator [12]. In order to make the control mode more flexible, some scholars have studied the control strategy based on open winding [13], and further developed the fault-tolerant control strategy [14]. And the control strategy of BDFRG under unbalanced grid voltage is proposed in [15],[16]. The above strategies are conventional power control strategies, aiming at the rapid response of power, so that the system can transmit more active current to the power grid as much as possible.

The continuous improvement of wind power permeability will lead to the decline of power system frequency stability. In order to avoid the resulting fault problems, wind farms are required to have some functions similar to traditional power plants, such as active power control, frequency regulation and dynamic voltage regulation [17]. VSG can control the active power of the system by simulating the rotor motion equation and power angle characteristics of synchronous generator, and control the reactive power by simulating the reactive power-voltage droop characteristics. Application of VSG control can change the external characteristics of power electronic equipment and improve the stability of power system [18]–[20].

In recent years, VSG strategy has been widely studied in photovoltaic power generation [21], multi-terminal flexible DC transmission systems [22]. In [23],[24], a control strategy for grid connected doubly fed wind turbines based on virtual synchronous control is proposed, which enhances the stability and 'inertia' of doubly fed wind turbines under weak grid conditions. However, there are no available reports about

Manuscript received July 08, 2022; revised December 07, 2022; accepted December 18, 2022. date of publication December 25, 2022; date of current version December 18, 2022.

This work was supported in part by the National Natural Science Foundation of China under Grant 51537007. *(Corresponding Author: Shi Jin)*

S. Liang is with Shenyang University of Technology, Shenyang, 110870, China (e-mail: 2209171334@qq.com).

S. Jin is with Shenyang University of Technology, Shenyang, 110870, China (e-mail: wby-js@163.com).

L. Shi is with Shenyang University of Technology, Shenyang, 110870, China (e-mail: 19147671555@qq.com).

Digital Object Identifier 10.30941/CESTEMS.2022.00052

BDFRG controlled with VSG.

This paper aims to fill the blank in the control strategy of BDFRG by introducing the concept, design content and simulation verification of BDFRG-VSG. The proposed BDFRG-VSG in this paper can make the system have the ability of frequency modulation and improve the adaptability of the system in the weak grid. Finally, in Matlab /Simulink, to verify the effectiveness and feasibility of the proposed strategy, variable-speed constant-frequency operation capability of BDFRG-VSG system is tested in ideal grid; and the BDFRG-VSG system is compared with the BDFRG-DPC system in the case of grid frequency mutation in simulation.

II. Mathematical Model of BDFRG

The stator of BDFRG has two sets of three-phase windings with different pole numbers: power winding and control winding. The power winding is directly connected to the power grid, and the control winding is connected to the power grid through the back-to-back converter. The reluctance rotor couples the magnetic field of two stator windings.

In the rotating reference frames, the voltage equation of BDFRG can be expressed as[1]

$$\begin{cases} \boldsymbol{U}_{\mathrm{p}} = R_{\mathrm{p}}\boldsymbol{I}_{\mathrm{p}} + \dfrac{\mathrm{d}\boldsymbol{\psi}_{\mathrm{p}}}{\mathrm{d}t} + \mathrm{j}\omega_{\mathrm{p}}\boldsymbol{\psi}_{\mathrm{p}} \\ \boldsymbol{U}_{\mathrm{c}} = R_{\mathrm{c}}\boldsymbol{I}_{\mathrm{c}} + \dfrac{\mathrm{d}\boldsymbol{\psi}_{\mathrm{c}}}{\mathrm{d}t} + \mathrm{j}(\omega_{\mathrm{p}} - \omega_{\mathrm{r}})\boldsymbol{\psi}_{\mathrm{c}} \end{cases} \tag{1}$$

Where $\boldsymbol{U}_{\mathrm{p}}$ and $\boldsymbol{U}_{\mathrm{c}}$ respectively represent the voltage of power winding and control winding, R_{p} and R_{c} are the resistance of power winding and control winding, $\boldsymbol{I}_{\mathrm{p}}$ and $\boldsymbol{I}_{\mathrm{c}}$ are the current of power winding and control winding, $\boldsymbol{\psi}_{\mathrm{p}}$ and $\boldsymbol{\psi}_{\mathrm{c}}$ is the flux linkage of power winding and control winding. The power winding reference frame rotates at ω_{p}, and the control winding reference frame rotates at ω_{c}.

In the rotating reference frames, the flux linkage equation of BDFRG can be expressed as[1,7]

$$\begin{cases} \boldsymbol{\psi}_{\mathrm{p}} = L_{\mathrm{p}}\boldsymbol{I}_{\mathrm{p}} + L_{\mathrm{m}}\hat{\boldsymbol{I}}_{\mathrm{c}} \\ \boldsymbol{\psi}_{\mathrm{c}} = L_{\mathrm{c}}\boldsymbol{I}_{\mathrm{c}} + L_{\mathrm{m}}\hat{\boldsymbol{I}}_{\mathrm{p}} \end{cases} \tag{2}$$

Where L_{p} and L_{c} are self inductance of power winding and control winding, L_{m} is mutual inductance between power winding and control winding, and superscript "^" represents conjugate vector.

The relationship between the angular velocity of the power winding (ω_{p}), the angular velocity of the control winding (ω_{c}) and the electrical angular velocity of the rotor (ω_{r}) is

$$\omega_{\mathrm{r}} = \omega_{\mathrm{p}} + \omega_{\mathrm{c}} \tag{3}$$

The active power (P_{p}) and reactive power (Q_{p}) of the power winding can be expressed as

$$P_{\mathrm{p}} + \mathrm{j}Q_{\mathrm{p}} = \frac{3}{2}\mathrm{Re}\left(\boldsymbol{U}_{\mathrm{p}}\hat{\boldsymbol{I}}_{\mathrm{p}}\right) + \mathrm{j}\frac{3}{2}\mathrm{Im}\left(\boldsymbol{U}_{\mathrm{p}}\hat{\boldsymbol{I}}_{\mathrm{p}}\right) \tag{4}$$

The electromagnetic torque (t_{e}) can be expressed as

$$t_{\mathrm{e}} = \frac{3}{2}P_{\mathrm{r}}\frac{L_{\mathrm{m}}}{L_{\mathrm{p}}}\left(\psi_{\mathrm{pd}}i_{\mathrm{cq}} + \psi_{\mathrm{pq}}i_{\mathrm{cd}}\right) \tag{5}$$

III. Virtual Synchronous Generator Control of BDFRG

In order to illustrate the frequency support principle of virtual synchronous generator, the response of BDFRG system based on conventional power control (CPC) is compared with that of synchronous generator (SG) under grid frequency disturbance.

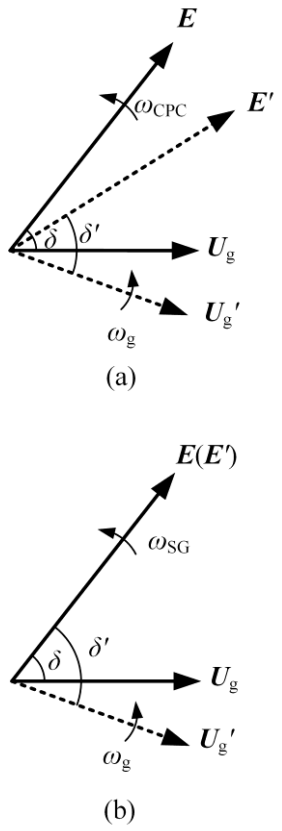

Fig. 1. Response comparison of grid frequency disturbance, (a): CPC; (b): SG.

In Fig. 1, (a) is the voltage vector diagram of BDFRG under conventional power control, (b) is the voltage vector diagram of synchronous generator. $\boldsymbol{E}$ and $\boldsymbol{U}_{\mathrm{g}}$ are generator internal potential and grid voltage before frequency disturbance, $\boldsymbol{E}'$ and U_{g}' are generator internal potential and grid voltage after frequency disturbance. δ is the angle between $\boldsymbol{E}$ and $\boldsymbol{U}_{\mathrm{g}}$, δ' is the angle between $\boldsymbol{E}'$ and $\boldsymbol{U}_{\mathrm{g}}'$. When the conventional power control is adopted, the internal potential phase of BDFRG always tracks the grid voltage phase; after the grid voltage phase mutation, the internal potential phase of BDFRG changes immediately, δ' is almost equal to δ; So power transmission is not affected by frequency disturbance, in other words, the system does not provide power to support the grid. On the contrary, due to the existence of rotating components in the synchronous generator, when the grid frequency changes, the internal voltage phase of the synchronous generator does not change immediately and δ increases to δ'; the active power transmitted to the grid also changes to help the grid frequency modulation. Therefore, by modifying the control strategy, the BDFRG system can simulate the characteristics of synchronous generators to help grid frequency regulation.

A. Overall Structure of BDFRG-VSG

The machine side converter (MSC) of BDFRG is responsible for regulating the power output of the system according to the reference value; the grid side converter (GSC) is responsible for maintaining constant DC bus voltage. Since the converter capacity of BDFRG is small and the DC bus capacitance is also small, the available energy is limited. The machine side converter can control the output of BDFRG, and the energy is considerable. Therefore, the proposed BDFRG control strategy is applied to the machine side converter. Main control structure of BDFRG-VSG is shown in Fig. 2.

VSG control adjusts the active and reactive power output by controlling the frequency and amplitude of the voltage. Therefore, in order to control the instantaneous value of U_p, it is necessary to establish the voltage source control of BDFRG. In Fig. 2, ω^* is provided by the virtual rotor motion equation, rather than the angular velocity of the grid. Because of the existence of line impedance, especially when the line impedance is inductive, the active power of BDFRG can be controlled by adjusting the frequency of the output voltage. Therefore, BDFRG may not always be synchronized with the grid. The amplitude and frequency of power winding voltage are no longer clamped by the power grid, but are determined by the virtual rotor motion equation and the virtual governor respectively, which can simulate the rotor motion equation and the reactive power-voltage droop characteristics. In this way, phase locked loop (PLL) is avoided in BDFRG-VSG.

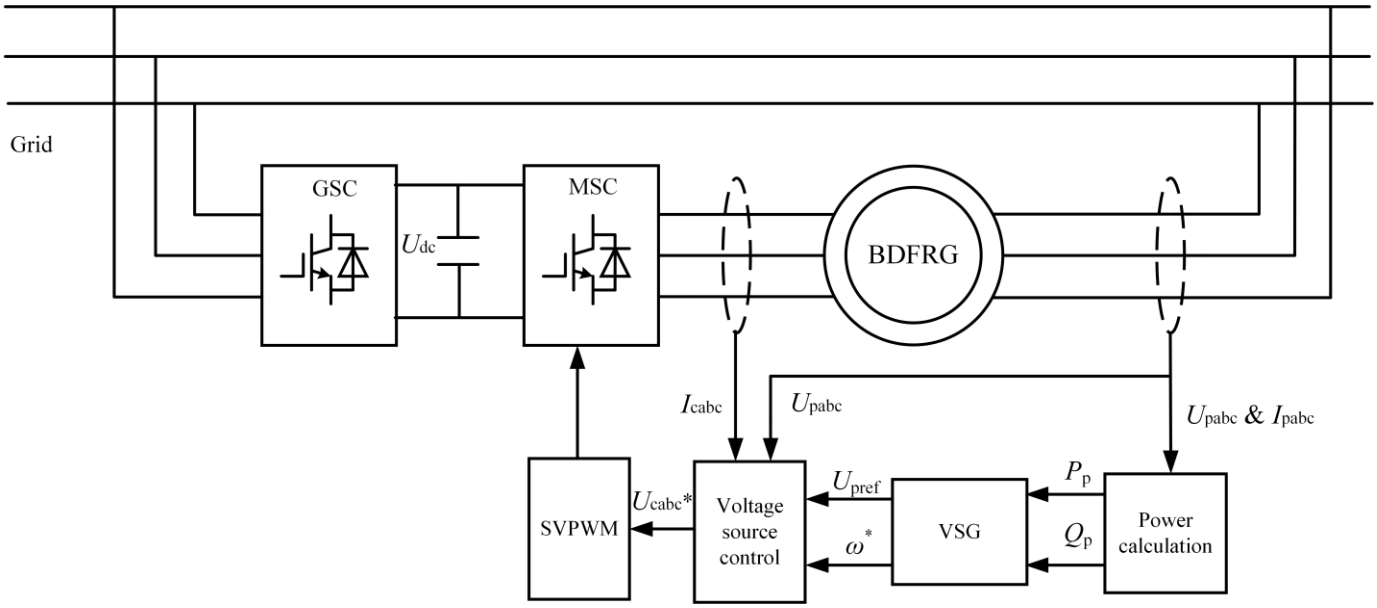

Fig. 2. Main control structure of BDFRG-VSG

In Fig. 2, U_{pabc} and I_{pabc} are the three-phase voltage and current of the power winding, and I_{cabc} is the three-phase current of the control winding. U_{pref} is the reference value of power winding voltage amplitude, ω^* is the reference value of frequency. P_p and Q_p can be expressed as

$$\begin{cases} P_p = \dfrac{3}{2}\left(u_{p\alpha} i_{p\alpha} + u_{p\beta} i_{p\beta}\right) \\ Q_p = \dfrac{3}{2}\left(u_{p\beta} i_{p\alpha} - u_{p\alpha} i_{p\beta}\right) \end{cases} \tag{6}$$

B. Voltage source control of BDFRG

In order to control the amplitude and frequency of power winding voltage, the voltage source control of BDFRG is established. The magnetic flux leakage coefficient is σ=1-L_m^2/(L_pL_s), (2) can be rewritten as

$$\boldsymbol{\psi}_c = L_c \boldsymbol{I}_c + L_m \hat{\boldsymbol{I}}_p = \sigma L_c \boldsymbol{I}_c + \frac{L_m}{L_p} \hat{\boldsymbol{\psi}}_p = \sigma L_p \boldsymbol{I}_p + \boldsymbol{\psi}_m \tag{7}$$

A simplified expression for the voltage of the control winding can be obtained by substituting (7) into (1),

$$\boldsymbol{U}_c = \mathrm{j}\omega_c \boldsymbol{\psi}_m + \left(R_c + \mathrm{j}\omega_c \sigma L_c\right) \boldsymbol{I}_c . \tag{8}$$

Equation (8) shows the relationship between the control winding voltage and current in vector sense. In scalar sense, i_{cd} is directly controlled by u_{cd}, and i_{cq} is directly controlled by u_{cq}. Therefore, the feedback loop can be constructed and the PI regulator can be used to control the current of the control winding.

In order to control output voltage of power winding directly, voltage closed loop control is adopted. When the load current is not considered, the voltage equation of the power winding can be expressed as

$$\begin{cases} u_{pd} = -\omega \psi_{pq} \\ u_{pq} = \omega \psi_{pd} \end{cases} \tag{9}$$

Accordingly, the flux linkage equation can be expressed as

$$\begin{cases} \psi_{pd} = L_m i_{cd} \\ \psi_{pq} = -L_m i_{cq} \end{cases} \tag{10}$$

The relationship between U_p and I_c can be obtained by substituting (10) into (9), as shown in

$$\begin{cases} u_{\mathrm{pd}} = \omega L_{\mathrm{m}} i_{\mathrm{cq}} \\ u_{\mathrm{pq}} = \omega L_{\mathrm{m}} i_{\mathrm{cd}} \end{cases} \tag{11}$$

According to (11), the q axis voltage of the power winding can be adjusted by the d axis current of the control winding, and the d axis voltage of the power winding can be adjusted by the q axis current of the control winding. The voltage source control block diagram of BDFRG is shown in Fig.3. Since the role of the GSC is to maintain the voltage stability of the DC bus, its control strategy is not the content of this paper, so it is not shown in Fig. 3. The converter in Fig. 3 is the machine side converter.

In the conventional power control strategy, the ideal grid is regarded as an ideal voltage source. But it should be noted that in this paper, the power winding is no longer regarded as directly connected to the ideal voltage source, but as indirectly connected to the ideal voltage source through line impedance. The voltage of the power winding is no longer clamped by the grid, which is closer to the actual situation. Therefore, on the premise of ensuring the stable operation of BDFRG system, the output voltage of power winding can be adjusted through voltage and current double closed loops.

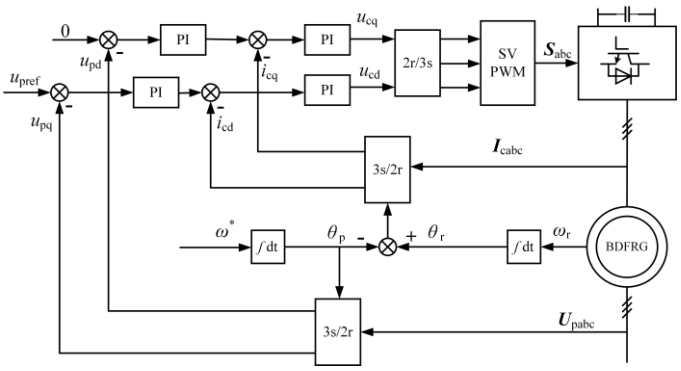

Fig. 3. Voltage source control block diagram of the BDFRG

C. Principle of virtual synchronous generator control

Many wind turbines are located in remote areas, where the grid is weak, so the grid-connected BDFRG system should have frequency modulation ability. By referring to the operating principle of governor of synchronous generator, the following can be obtained,

$$P_{\mathrm{m}} = P_{\mathrm{ref}} + \mathrm{K}_{\omega}(\omega_0 - \omega) \tag{12}$$

Where P_{m} is the mechanical power output from the prime mover, P_{ref} is active power reference of power winding, ω_0 is the grid angular frequency reference, ω is the angular frequency of the power winding, and K_{ω} is the frequency modulation coefficient. K_{ω} reflects the change value of VSG input power when the grid frequency changes by 1Hz, as expressed in

$$\mathrm{K}_{\omega} = -\frac{\Delta P}{\Delta f} \tag{13}$$

Referring to the electromagnetic equation and rotor motion equation of synchronous generator, the rotor motion equation of VSG can be expressed as

$$(P_{\mathrm{m}} - P_{\mathrm{p}}) - \mathrm{D}(\omega^* - \omega_0) = \mathrm{J}_{\mathrm{v}}\omega_0 \frac{\mathrm{d}\omega^*}{\mathrm{d}t} \tag{14}$$

Where P_{p} is the instantaneous value of the active power of the power winding, and D is the damping coefficient, ω^* is the power winding angular frequency reference, and J_{v} is the virtual inertia. D can be expressed as

$$\mathrm{D} = -\frac{\Delta T_{\mathrm{e}}}{\Delta\omega} = \frac{\mathrm{K}_{\omega}}{2\pi\omega_{\mathrm{n}}} \tag{15}$$

The relationship between J_{v} and D can be expressed as

$$\mathrm{J}_{\mathrm{v}} = \tau\mathrm{D} \tag{16}$$

Where τ is the time constant. To ensure the sensitivity of the system to frequency changes, τ can be appropriately smaller. The larger the value of J_{v}, the stronger the system inertia, the smaller the change of frequency per unit time, and the longer the time to reach stability. Increasing D will reduce the overshoot of power and frequency, but will slow down the response speed of the system. At the same time, D also has the function of droop adjustment. Therefore, it is necessary to balance the advantages and disadvantages of all aspects and make a compromise correction for J_{v} and D.

The traditional synchronous generator adjusts the output voltage and reactive power by changing the excitation. Similarly, the following can be obtained,

$$U_{\mathrm{pref}} = U_0 + \frac{1}{\mathrm{K}_{\mathrm{q}}}(Q_{\mathrm{pref}} - Q_{\mathrm{p}}) \tag{17}$$

Where U_{pref} is the reference value of voltage source control, U_0 is the grid voltage, K_{q} is the voltage regulation coefficient, Q_{pref} is the reactive power setting value of the power winding, and Q_{p} is the instantaneous value of reactive power of power winding. K_{q} can be expressed as

$$\mathrm{K}_{\mathrm{q}} = -\frac{\Delta Q}{\Delta U} \tag{18}$$

It should be noted that only when the line impedance of the system is inductive, the corresponding relationship between active power-frequency and reactive power-voltage will be established. If the line resistance is large, this regulation relationship will not be established, resulting in active power and reactive power coupling. Therefore, the system impedance is assumed to be inductive in this paper.

The specific structure of VSG control is shown in Fig. 4.

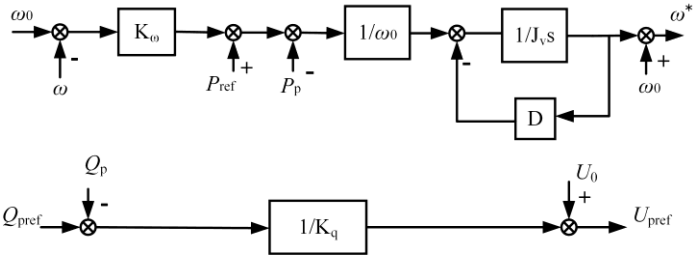

Fig. 4. Structure of VSG control

IV. Simulation Results

The BDFRG-VSG control strategy mentioned in this paper was validated in Matlab/Simulink. The BDFRG parameters are

shown in Table I.

TABLE I
BDFRG PARAMETERS

Parameters	Value
Rated voltage (V)	380
Rated frequency (Hz)	50
Rated power (kW)	25
Pole-pairs of power winding	4
Pole-pairs of control winding	2
Power winding resistance (Ω)	0.3871
Control winding resistance (Ω)	0.3773
Power winding self-inductance (mH)	47.66
Control winding self-inductance (mH)	40.75
Mutual inductance (mH)	37.68

The simulation parameters of BDFRG-VSG are shown in Table II.

TABLE II
SIMULATION PARAMETERS

Parameters	Value
DC voltage (V)	300
Grid rated voltage (V)	380
Switch frequency (kHz)	10
Frequency modulation coefficient K_ω	4710
Voltage regulation coefficient K_q	40
Virtual inertia J_v (kg/m^2)	0.8
Damping coefficient D (N/(m/s))	8
Line resistance (Ω)	0.1
Line inductance (mH)	8

A. Simulation in Ideal Grid

BDFRG is integrated into the grid at 1s, the active power reference of the power winding increases from -8kW to -14kW at 1s, and increases to -18kW at 2s (negative sign '-' means generating active power). To ensure unit power operation, reactive power reference is 0. In order to verify the variable-speed constant-frequency operation capability of BDFRG-VSG, the reference rotor speed increase from 450r/min to 550r/min uniformly within 1s-3s, as shown in Fig. 5. At this time, BDFRG transits from sub-synchronous operation state to synchronous operation state, and then to super-synchronous operation state.

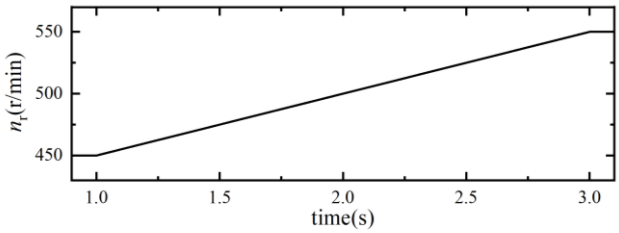

Fig. 5. Rotor speed reference

Fig. 6 is the simulation results of BDFRG-VSG in ideal grid. In Fig. 6, (a) is the power winding three-phase voltage waveform (U_p), (b) is the power winding three-phase current waveform (I_p), (c) is the active power waveform of the power winding (P_p), (d) is the reactive power waveform of the power winding (Q_p), (e) is the voltage frequency waveform of the power winding (f_p) measured by the PLL, (f) is the q-axis voltage waveform of the power winding (U_{pq}) in the two-phase synchronous rotating coordinate system, (g) is the waveform of electromagnetic torque (t_e), and (h) is the control winding three-phase current waveform (I_c).

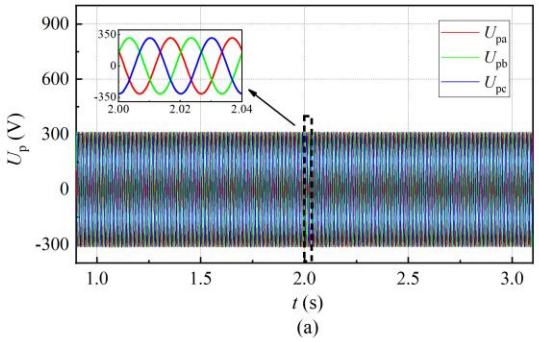

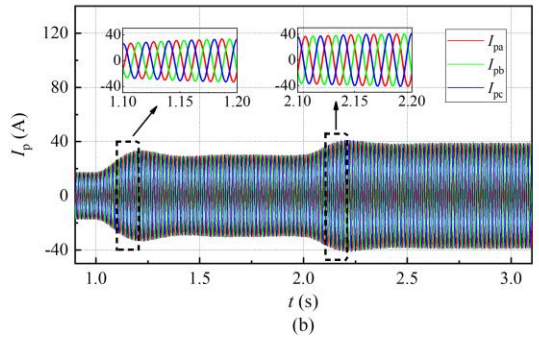

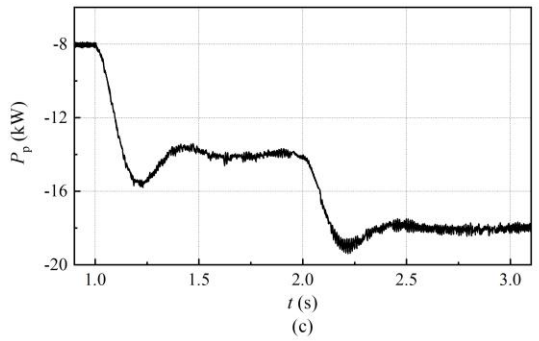

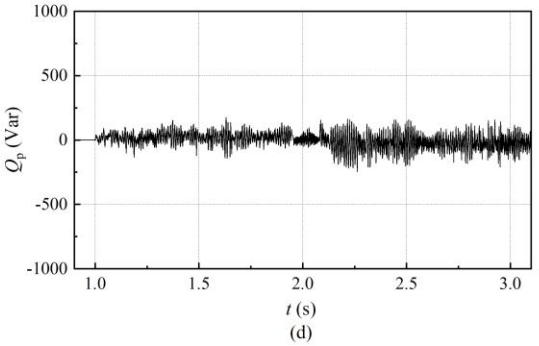

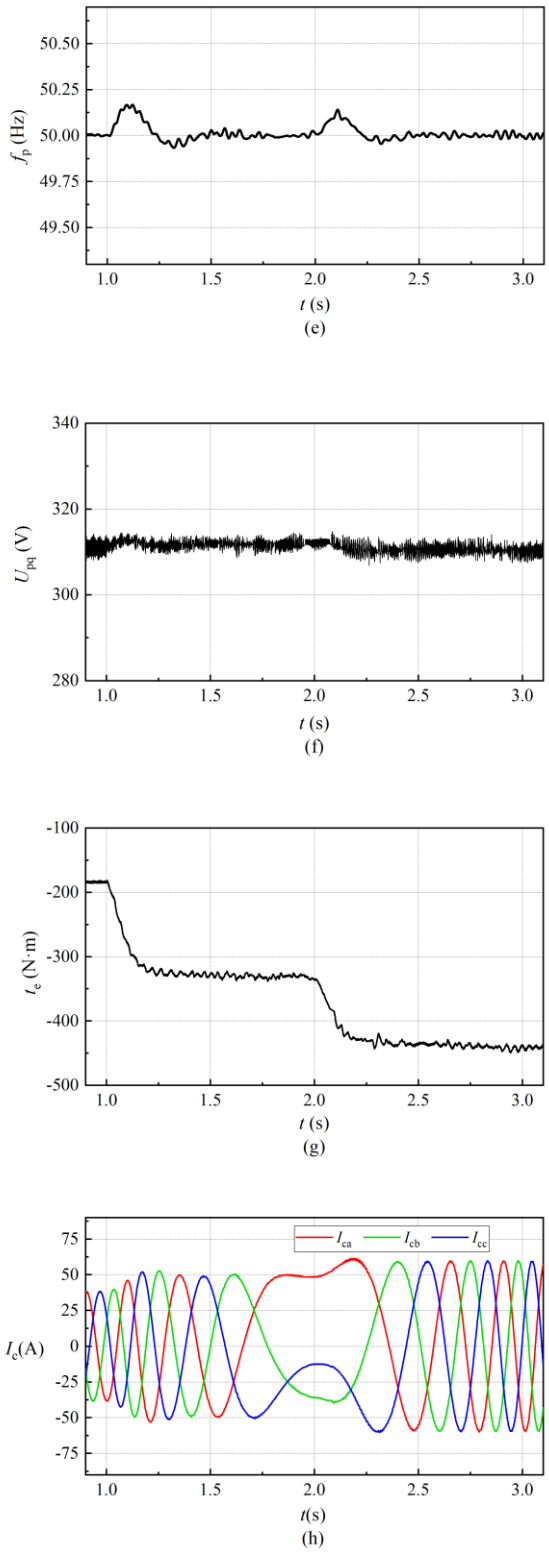

Fig. 6 Dynamic response simulation results of BDFRG-VSG, (a)U_p; (b) I_p; (c) P_p; (d) Q_p; (e) f_p; (f) u_{pq}; (g) t_e; (h) I_c.

Fig. 6 shows the operating condition of BDFRG-VSG after grid-connected. BDFRG-VSG can operate stably in sub-synchronous speed, synchronous speed and super-synchronous speed. P_p can follow the reference smoothly, Q_p remains at 0. when P_p increases, the impact on Q_p is small, and the decoupling of P_p and Q_p is realized. It can be seen from the waveform of f_p that after the change of P_p reference, f_p change first , and then the P_p of the system increase gradually , which is reflected in a relatively slow adjustment process with 'inertia', reflecting the corresponding relationship between active power and frequency. By observing the waveforms of Q_p and U_{pq}, the increase of P_p has a certain effect on Q_p, and U_{pq} changes with Q_p, reflecting the corresponding relationship between reactive power and voltage. The trend of I_p amplitude is consistent with the P_p. With the increase of P_p, the amplitude of I_c increases; with the change of rotor speed, the frequency of I_c first decreases and then increases gradually; and the I_c can be adjusted according to the operation state and power reference changes of BDFRG.

B. *Frequency Variation Disturbance Simulation*

In order to verify the support ability of BDFRG-VSG to the grid frequency, a comparative simulation is carried out for the described BDFRG-VSG and the onventional power control strategy of BDFRG-DPC in the case of grid frequency mutation. The simulation results are shown in Fig. 7 and Fig. 8. System parameters are consistent with the simulation in ideal grid. The active power reference of BDFRG-VSG and BDFRG-DPC is -14kw, and the speed is fixed at 550r/min.

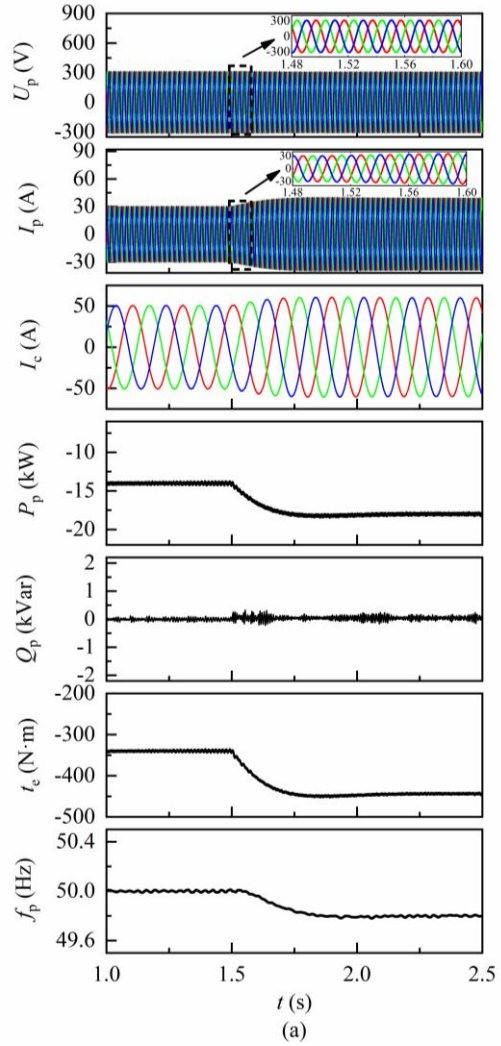

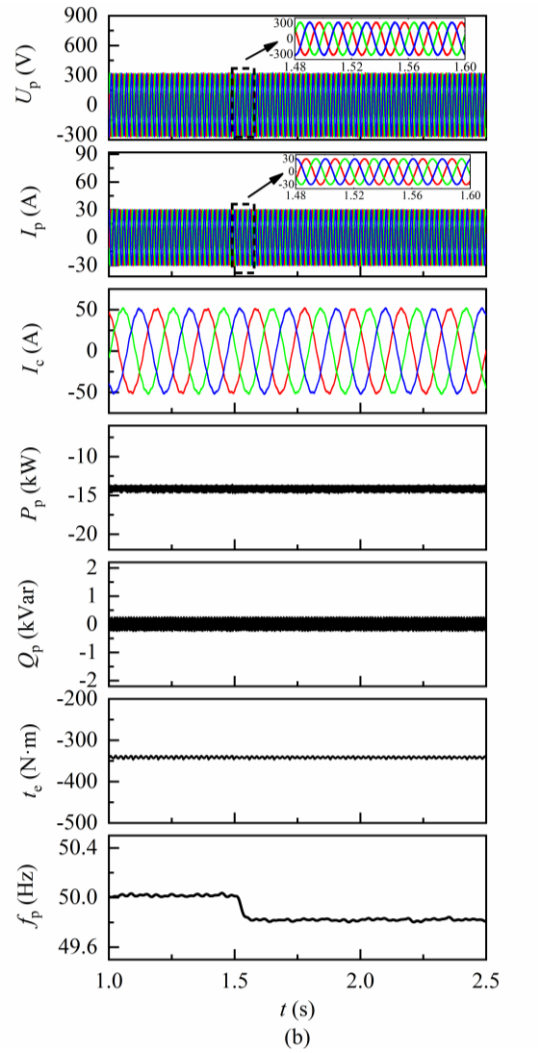

Fig. 7. Simulation results of grid frequency dropping to 49.8Hz, (a) BDFRG-VSG; (b) BDFRG-DPC.

Firstly, the responses of the two systems in the case of sudden frequency drop are simulated. At 1.5s, the grid frequency the grid frequency decreases from 50 Hz to 49.8 Hz. The simulation results are shown in Fig. 7.

Fig. 7 shows that BDFG-VSG and BDFG-DPC can operate well. Before the grid frequency drop, active power and reactive power can follow their reference values. The electromagnetic torque waveform is stable, and the current of power winding and control winding is sinusoidal and balanced. The steady-state characteristics of the two control methods are basically consistent.

Fig. 7(a) shows that, when the grid frequency drops to 49.8Hz, BDFRG-VSG outputs an additional 4kW active power to help the grid complete the frequency modulation. The trend of I_p amplitude is consistent with P_p. Since the electromagnetic torque belongs to the resistance torque, its waveform is negative. When the grid frequency drops suddenly, the amplitude of the electromagnetic torque increases. The frequency of power winding voltage does not change immediately due to the action of virtual rotor motion equation, and it transits to the grid frequency after 0.4s, which reflects the 'inertia' of the BDFRG-VSG system.

Fig. 7(b) shows that P_p and t_e of BDFRG-DPC are not affected when the grid frequency drops to 49.8Hz. The frequency of power winding keeps consistent with the grid frequency quickly, and the transition process is only about 0.05s. Since the PLL requires a certain response time, the actual transition process is less than 0.05s. Therefore, it can be considered that the 'inertia' of BDFRG-DPC system is far less than that of BDFRG-VSG system. Simulation results are consistent with theoretical analysis.

The active power reference still is -14kw, and the speed is fixed at 550r/min. The grid frequency increases from 50Hz to 50.2Hz at 1.5s. Figure 8 shows the simulation results of BDFRG-VSG and BDFRG-DPC when the grid frequency suddenly increases to 50.2Hz, where (a) is the simulation results of BDFRG-VSG and (b) is the simulation results of BDFRG-DPC.

Fig. 8(a) shows that P_p of BDFRG-VSG decreases by 4 kW, after the grid frequency increases to 50.2 Hz, so as to help the grid frequency modulation. Accordingly, the t_e and I_p also decrease. The power winding frequency takes about 0.4 s to transition to the grid frequency.

Fig. 8(b) shows that the transition time of BDFRG-DPC is still very short. It lacks the ability to support grid frequency.

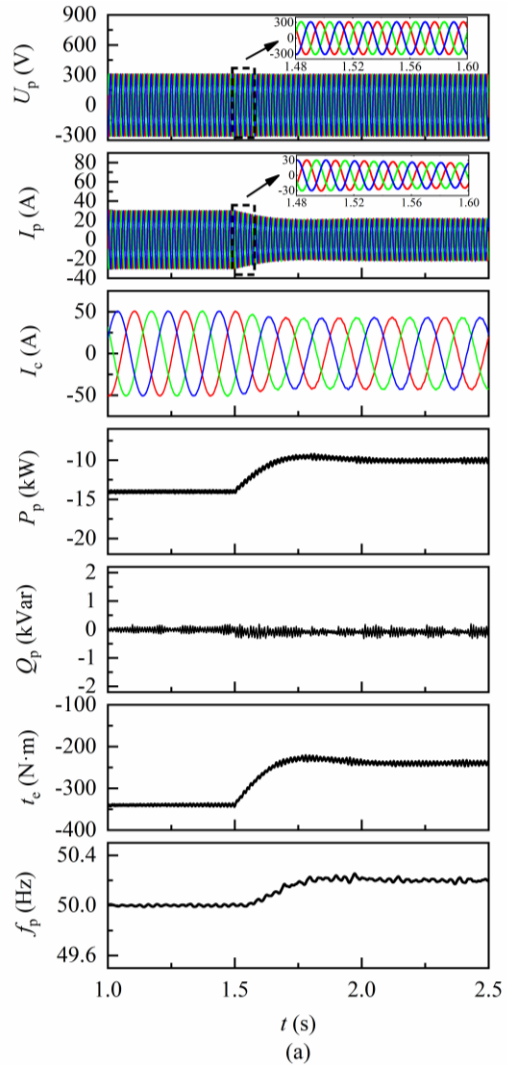

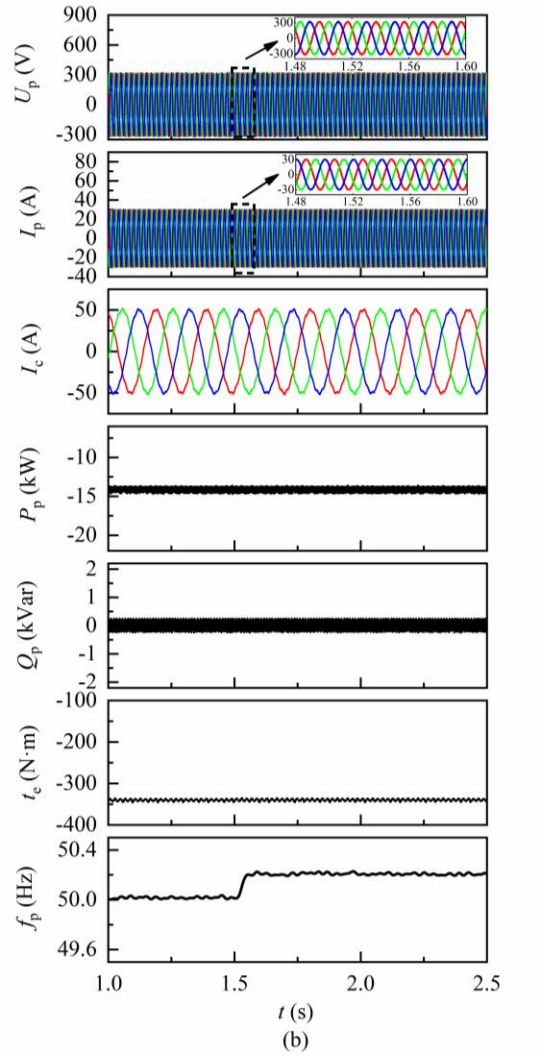

Fig. 8. Simulation results of power grid frequency increasing to 50.2Hz, (a) BDFRG-VSG; (b) BDFRG-DPC.

V. CONCLUSION

The BDFRG system based on the conventional power control strategy cannot take responsibility for frequency stability, a BDFRG control strategy based on virtual synchronous generator is proposed in this paper. The control strategy has versatility and does not depend on PLL. The most important feature is that the strategy can support the frequency of the grid and has grid friendliness. The simulation results show that the BDFRG-VSG control strategy proposed in this paper can smoothly control the active power and reactive power; and BDFRG-VSG can respond to the change of grid frequency and adjust the active power output to support grid frequency.

REFERENCES

[1] S. Ademi and M. Jovanovic, "High-efficiency control of brushless doubly-fed machines for wind turbines and pump drives," *Energy Conversion & Management*, vol. 81, pp. 120-132, May 2014.

[2] O. Sadeghian, S. Tohidi, B. Mohammadi-Ivatloo, and F. Mohammadi, "A Comprehensive Review on Brushless Doubly-Fed Reluctance Machine," *Sustainability*, vol. 13, no. 2, Jan 2021, Art no. 842.

[3] M. Kumar, S. Das, and K. Kiran, "Sensorless Speed Estimation of Brushless Doubly-Fed Reluctance Generator Using Active Power Based MRAS," *IEEE Transactions on Power Electronics*, vol. 34, no. 8, pp. 7878-7886, Aug 2019.

[4] D. Gay, R. E. Betz, D. Dorrell, and A. Knight, "Grid Fault Performance of Brushless Doubly-Fed Reluctance Machines in Wind Turbine Applications," in *Proceedings of 20th European Conference on Power Electronics and Applications* , Riga, LATVIA, 2018, pp. 1-10.

[5] F. X. Wang, F. G. Zhang, and L. Y. Xu, "Parameter and performance comparison of doubly fed brushless machine with cage and reluctance rotors," *IEEE Transactions on Industry Applications.*, vol. 38, no. 5, pp. 1237-1243, Sep-Oct 2002.

[6] M. G. Mousa, S. M. Allam, and E. M. Rashad, "A comparative study of vector-control strategies for maximum wind-power extraction of a grid-connected wind-driven brushless doubly-fed reluctance generator," *Australian Journal of Electrical & Electronics Engineering*, vol. 14, no. 1-2, pp. 1-11, 2017.

[7] S. Ademi and M. G. Jovanovic, "Vector Control Methods for Brushless Doubly Fed Reluctance Machines," *IEEE Transactions on Industrial Electronics*, vol. 62, no. 1, pp. 96-104, Jan 2015.

[8] M. R. A. Kashkooli and M. G. Jovanovi, "Sensorless adaptive control of brushless doubly-fed reluctance generators for wind power applications," *Renewable Energy*, vol. 177, pp. 932-941, Nov 2021.

[9] H. Chaal and M. Jovanovic, "Toward a Generic Torque and Reactive Power Controller for Doubly Fed Machines," *IEEE Transactions on Power Electronics*, vol. 27, no. 1, Jan 2012.

[10] M. Jovanovic, "Sensored and sensorless speed control methods for brushless doubly fed reluctance motors," *Iet Electric Power Applications*, vol. 3, no. 6, pp. 503-513, Nov 2009.

[11] H. Chaal and M. Jovanovic, "Direct Power Control of Brushless Doubly-Fed Reluctance Machines," in *Proceedings of 5th IET International Conference on Power Electronics, Machines and Drives*, Brighton, UK, 2010, pp. 1-6.

[12] M. Moazen, R. Kazemzadeh, and M.-R. Azizian, "Model-based predictive direct power control of brushless doubly fed reluctance generator for wind power applications," *Alexandria Engineering Journal*, vol. 55, no. 3, pp. 2497-2507, Sep 2016.

[13] F. Zhang, L. Zhu, S. Jin, X. Su, S. Ademi, and W. Cao, "Controller Strategy for Open-Winding Brushless Doubly Fed Wind Power Generator With Common Mode Voltage Elimination," *IEEE Transactions on Power Electronics*, vol. 66, no. 2, pp. 1098-1107, Feb 2019.

[14] S. Jin, L. Shi, Y. Zhang, D. Sun, and B. Ji, "Fault-tolerant control strategy of open-winding brushless doubly fed wind power generator based on direct power control," *IET Electric Power Applications*, vol. 15, no. 7, pp. 799-810, Jul 2021.

[15] M. Moazen, R. Kazemzadeh, and M. Azizian, "A model-based PDPC method for control of BDFRG under unbalanced grid voltage condition using power compensation strategy," *Journal of Operation and Automation in Power Engineering*, vol. 8, no. 2, pp. 128-140, 2020.

[16] T. Taluo, L. Ristic, and M. Jovanovic, "Dynamic Modeling and Control of BDFRG under Unbalanced Grid Conditions," *Energies*, vol. 14, no. 14, Jul 2021, Art no. 4297.

[17] C. Sourkounis and P. Tourou, "Grid Code Requirements for Wind Power Integration in Europe," in *Proceedings of Conference Papers in Energy*, 2013, pp. 1-9.

[18] Q.-C. Zhong and G. Weiss, "Synchronverters: Inverters That Mimic Synchronous Generators," *IEEE Trans. Ind. Electron.*, vol. 58, no. 4, pp. 1259-1267, Apr 2011.

[19] J. Alipoor, Y. Miura, and T. Ise, "Power System Stabilization Using Virtual Synchronous Generator With Alternating Moment of Inertia," *IEEE Journal of Emerging and Selected Topics in Power Electronics*, vol. 3, no. 2, pp. 451-458, Jun 2015.

[20] S. Dong and C. Chen, "A Method to Directly Compute Synchronverter Parameters for Desired Dynamic Response," in *Proceedings of 2018 IEEE Power & Energy Society General Meeting (PESGM)*, 2018, pp. 1-1.

[21] A. Hosseinipour and H. Hojabri, "Virtual inertia control of PV systems for dynamic performance and damping enhancement of DC microgrids with constant power loads," *IET Renewable Power Generation*, vol. 12, no. 4, pp. 430-438, Mar 19 2018.

[22] Y. J. Cao et al., "A Virtual Synchronous Generator Control Strategy for VSC-MTDC Systems," *IEEE Transactions on Energy Conversion*, vol. 33, no. 2, pp. 750-761, Jun 2018.

[23] S. Wang, J. Hu, X. Yuan, and L. Sun, "On Inertial Dynamics of Virtual-Synchronous-Controlled DFIG-Based Wind Turbines," *IEEE*

Transactions on Energy Conversion, vol. 30, no. 4, pp. 1691-1702, Dec 2015.

[24] Y. Y. Zhao, J. Y. Chai, X. D. Sun, and Ieee, "Virtual Synchronous Control of Grid-Connected DFIG-based Wind Turbines," in *Proceedings of 30th Annual IEEE Applied Power Electronics Conference and Exposition*, Charlotte, NC, 2015, pp. 2980-2983.

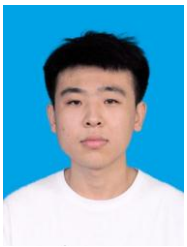

Shuai Liang was born in Shandong, China, in 1999. He received the B.S. degree in electrical engineering from the Shenyang University of Technology in 2019. He is currently pursuing the M.S. degree in electrical engineering from Shenyang University of Technology since 2021.

His research interests include wind power generators and their control.

Shi Jin (M'17) was born in 1981. She received the B.E., M.S., and Ph.D. degrees from Shenyang University of Technology, Shenyang, China, in 2004, 2007, and 2011, respectively, all in electrical engineering.

She is a professor at the School of Electrical Engineering, Shenyang University of Technology. Her research and teaching interests mainly include power electronic technology, electrical machines and their control systems, and wind power generation. For the last several years, she has undertaken two research projects supported by the National Natural Science Foundation of China, and has won five provincial and ministerial science and technology awards. She has authored or coauthored 73 papers published in important academic journals and presented at domestic and international conferences, of which 57 were cited by SCI/EI. She was selected as "Baiqianwan Talents Project of Liaoning Province" in 2019 and the academic leader of Shenyang University of Technology in 2015.

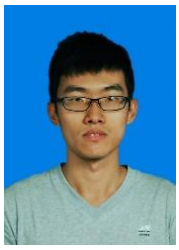

Long Shi received the B.S. and M.S. degrees in electrical engineering from the Shenyang University of Technology, Shenyang, China, in 2015 and 2018. He is currently working toward the Ph.D. degree from the College of Electrical Engineering, Shenyang University of Technology. His research interests include motors and their control, and wind power generators and their control.